Experimental Determination of Ca-Silicate Dissolution Rates: A Source of Calcium for Geologic CO_2 Sequestration

Susan A. Carroll (carroll6@llnl.gov; 925-423-5694)
Energy and Environment Directorate
Lawrence Livermore National Laboratory
L-219
Livermore, CA 94550

Kevin G. Knauss (knauss@llnl.gov; 925-422-1372)
Energy and Environment Directorate
Lawrence Livermore National Laboratory
L-219
Livermore, CA 94550

Introduction

The international scientific community recognizes that greenhouse gases have the potential to influence climate, and that potential changes in sea level and weather patterns would be largely deleterious. Because CO_2 is emitted in such large quantities and its atmospheric concentration has been consistently rising throughout the recent past, it is only prudent to focus attention on reducing its emission and on developing strategies for its removal from the atmosphere [1]. A variety of removal methods have been suggested ranging from deep-sea disposal, to recycling to methanol, and to conversion to solid carbonate [2]. Problems appear to remain with all these strategies, and more work is needed to develop an acceptable, efficient method or set of methods.

The idea of converting the gas to solid carbonate is particularly appealing, because on a human time scale, this is permanent disposal. The reaction of CO_2 and water with unstable silicate minerals to produce more stable silicates (e.g., clays) and solid carbonates is the natural weathering process which is a dominant part of the long-term global geochemical cycling process (e.g., [3]). The Earth's large deposits of limestone and dolomite (the two primary forms of carbonate rock) represent the Earth's natural response to volcanic CO_2 emissions over much of planetary history. Recently, the suggestion was made to utilize the reaction of CO_2 with silicate minerals that occurs naturally during chemical-weathering within deep sedimentary basins[4] or in aquifers [1] as a basis for removal.

Problem

Geologic sequestration of CO_2 appears to be most promising, because it is simply mimicking nature by using the same method to dispose of CO_2 that the Earth itself uses to regulate climate. For an aquifer injection process to be successful, a careful balance needs to be made among the rate of injection, the rate of local groundwater flow, and the rates of specific chemical reactions. This is achievable only with the use of detailed geochemical computer models. Accurate knowledge of chemical reaction rates in multi-mineral systems is important, because physical flow will be affected by changes in formation porosity and permeability. Acid water near the injection well will dissolve silicate and calcium minerals and increase porosity and permeability. As the acid plume is neutralized by mineral dissolution, carbonate and clay minerals will precipitate further away from the injection well. There is a lack of experiments that measure the coupled dissolution and precipitation reactions of multi-mineral systems, and there are no experimental studies of the direct effects of high levels of dissolved carbon on silicate and carbonate reaction kinetics.

Solution

Our approach is to conduct single and multi-mineral dissolution and precipitation experiments in the Ca-Al-Si-CO_2 system as a function of pCO_2, pH and temperature. Our kinetic research will feed directly into reactive transport codes that can evaluate aquifer storage of dissolved CO_2 and mineral carbonates, and resulting changes in porosity and permeability.

Project Description

We have experimentally measured the rate of labradorite dissolution ($Ca_{0.6}Na_{0.4}Al_{1.6}Si_{2.4}O_8$) in waters saturated with supercritical CO_2 (pCO_2 = 1400 psi, CO_2 (aq) = 0.6 molal, pH 3.2) at 30, 60, and 100ºC using mixed flow reactors. These experiments simulate the reactive front of supercritical CO_2 and aquifer water. They are designed to investigate the available source of calcium for storage of CO_2 as carbonates and the source of aluminum and silica for the precipitation of secondary minerals that will effect aquifer porosity and permeability. To determine the direct effect of elevated CO_2 on mineral dissolution we also conducted labradorite dissolution experiments in dilute HCl solutions (pH 3.2) saturated with atmospheric CO_2 at 30, 60, 100 and 130ºC. The experimental conditions are shown in Table 1.

Experimental System

Figure 1 is a schematic drawing of our experimental system that allows us to investigate reaction kinetics in water equilibrated with supercritical CO_2 over a range of temperature and pressure. The system consists of two reactors. A static titanium pressure vessel is used to equilibrate water with supercritical CO_2 (# 2) and a titanium mixed flow reactor is used to dissolve the calcium silicate minerals (# 3). All parts of the reactors that contact the hot aqueous solution are made of passivated titanium, which forms highly insoluble TiO_2 on the surface (some of the pumping is made of Hastalloy C0276 and Nitronics-50 steel, which are inert in our solutions). In the mixed flow reactor vessel, the calcium-feldspar is placed between two titanium screens separated by a spacer just below the stirring rod. We included a single cleaved feldspar crystal

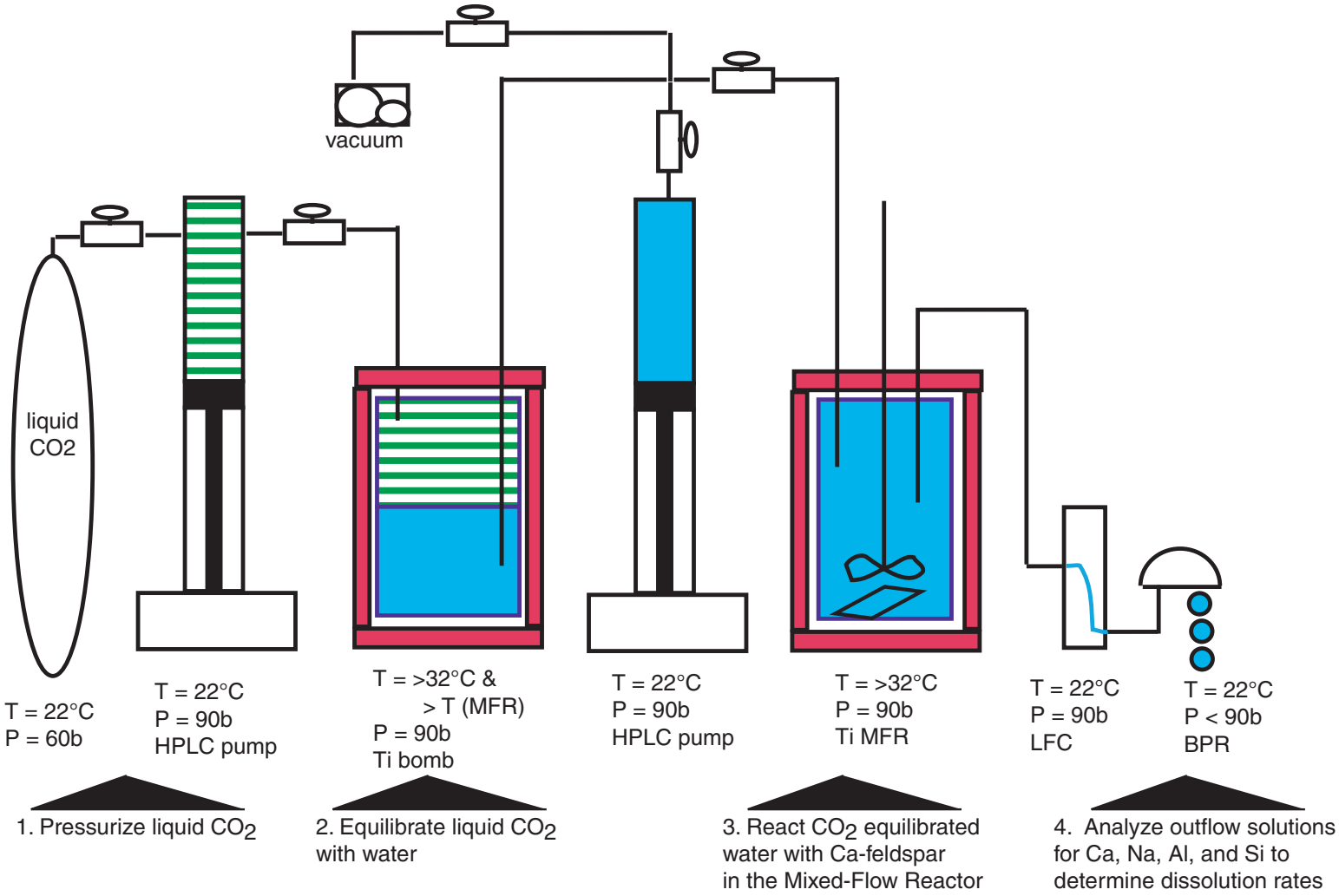

Figure 1. Mineral dissolution at elevated CO_2 in a mixed flow reactor

Table 1. Labradorite Dissolution Experiments in waters saturated supercritical CO_2 and with atmospheric CO_2. *pH is calculated from the measured dissolved CO_2 . All other pH were measured at room temperature. Stacked experiments are shown by like superscripts.

Run No.	$CO_{2\,(aq)}$	pH	T°C	Flow Rate	Log Dissolution Rate (mol Labradorite cm^{-2} s^{-1})			
				(ml/min)	Na	Ca	Al	Si
An60-60-1000	0.71±0.02	3.2*	61	1.0	-11.86±0.03	nd	-12.73±0.08	-12.37±0.03
An60-150-1400 (2)	0.66±0.03	3.5*	150	1.0	-12.06±0.02	-11.77±0.01	ppt	-11.18±0.02
[1]An60-30-1400	0.61±0.07	3.2*	31	0.86	-12.58±0.02	-13.19±0.05	-13.05±0.02	-13.45±0.01
[1]An60-60-1400	0.61±0.07	3.2*	60	0.87	-12.34±0.01	-12.77±0.03	-12.67±0.01	-13.02±0.02
[1]An60-100-1400	0.61±0.07	3.2*	100	0.85	-12.30±0.01	-12.34±0.03	-12.34±0.01	-12.34±0.03
[2]An60-30-0 (1)		3.21	30	0.88	-12.68±0.25	-13.07±0.14	-13.15±0.07	-13.53±0.05
[2]An60-60-0 (2)		3.29	60	0.88	-12.38±0.22	-12.45±0.27	-12.75±0.04	-12.83±0.03
[2]An60-100-0 (1)		3.29	100	0.88	-12.22±0.08	-12.49±0.09	-12.31±0.01	-12.31±0.01
[2]An60-100-0 (2)		3.24	100	4.3	-12.06±0.01	-12.28±0.01	-12.14±0.02	-12.11±0.01
[2]An60-100-0 (3)		3.37	100	0.22	-12.41±0.10	-12.57±0.01	-12.55±0.02	-12.52±0.01
[2]An60-100-0 (4)		3.25	100	8.7	-12.44±0.31	-11.90±0.07	-11.97±0.07	-12.09±0.01
[2]An60-130-0 (1)		3.22	130	8.60	-11.58±0.12	-11.69±0.04	-11.95±0.06	-11.67±0.01
[2]An60-130-0 (2)		3.24	130	4.32	-11.40±0.07	-11.86±0.04	-12.85±0.30	-11.66±0.03
[2]An60-130-0 (3)		3.30	130	0.88	-11.63±0.02	-11.69±0.01	-13.08±0.07	-11.72±0.01

for post-mortem atomic force microscopy analyses, in addition to the high surface area, ground feldspar (surface area = 0.03 m^2 g^{-1}). After pulling a vacuum on the entire system, both reactors are filled with distilled and deionized water using a HPLC pump, and brought to experimental run temperature and pressure. Supercritical CO_2 is made by pressurizing liquid CO_2 in a HPLC pump to about 90 bar at room temperature (# 1). The supercritical CO_2 is pumped into the static reactor (and some water is displaced to the second HPLC pump), and then equilibrated with distilled and deionized water at a temperature above the temperature in the mixed flow reactor to keep the CO_2 dissolved in the aqueous phase throughout the entire system (#2). We

typically equilibrate the water with supercritical CO_2 overnight, but equilibration occurs easily within a couple of hours. The CO_2 equilibrated water is the input solution for the dissolution experiment and is continually pumped through the mixed flow reactor containing the calcium-feldspar (#3). A siphon tube at the bottom of the static reactor ensures that water and not supercritical CO_2 is pumped through the mixed flow reactor. Flow rates are controlled with the supercritical CO_2 HPLC-syringe pump, which displaces the water from the static reactor to the mixed flow reactor. At the sampling port on the downstream side of the backpressure regulator, the outflow solution degasses at atmospheric pressures. We have developed a protocol to measure CO_2 by extracting the sample directly into a gas tight syringe loaded with concentrated NaOH. The CO_2 is effectively trapped as dissolved carbonate until it is analyzed with a carbon analyzer. Degassed samples are collected for pH, Al, Ca, Na, and Si analyses by ICP-AES. For the atmospheric CO_2 experiments, the 6.5×10^{-4} M HCl solution was pumped directly into the mixed flow reactor with an HCLP pump.

The mix flow reactor is a state-of-the-art reaction vessel for mineral kinetic studies. The flow through design allows the net mineral dissolution and precipitation rates to be determined from the change in inflow and outflow solution composition, Δ[Na, Ca, Al, or Si], the flow rate (FR) and the mineral surface area, A,

$$\text{Net Rate} \propto \Delta[\text{Na, Ca, Al, or Si}] * FR*A \qquad 1.$$

Our experiments were conducted as a series of stacked runs at variable temperature and flow rate with the same solid sample. The flow-through design allows the reactions kinetics to be studied as a function of the solution composition and reaction affinity (or the Gibb's free energy of reaction, ΔG_r). We anticipate that reaction affinity will be an important parameter for kinetic reactions within an aquifer chosen for CO_2 sequestration, because the dissolution and precipitation reactions will approach equilibrium.

Labradorite growth and dissolution features were imaged ex-situ with an atomic force microscope (Digital Instruments, AFM/LRM) at room temperature on single cleaved crystals recovered at the end of the stacked runs. As such, images record a history of dissolution

environments because the mixed-flow reactor experiments contained several stacked runs carried out on the same mineral sample at different temperatures and flow rates. We plan to conduct in-situ experiments at elevated temperature and pressure using the hydrothermal atomic force microscope in the future [5, 6].

Results

Effect of elevated CO_2 on labradorite dissolution

Figure 2a compares labradorite dissolution rates from experiments with water saturated with respect to 1400 psi CO_2 and atmospheric CO_2 from 30 to 130°C at pH 3.2. The rates shown in are normalized to molar Al, Si, Ca, and Na found in labradorite. At the reactive front of a supercritical CO_2 plume equilibrating with aquifer water, mineral dissolution rates will be enhanced over the ambient ground water, because the water will have a high acid content from dissolved CO_2. Acid water hydrolyzes the mineral surface, breaking framework bonds, resulting in mineral dissolution [7]. We observed no direct effect of dissolved CO_2 on labradorite dissolution. Labradorite dissolution rates measured at pH 3.2 with much lower dissolved CO_2 are the same. The only difference between these two sets of experiments is the acid source. In the experiments with water equilibrated with supercritical CO_2, 0.6 M of dissolved CO_2 creates a pH 3.2 water, and in the experiments with waters in equilibrium with atmospheric CO_2, HCl is added to the water to yield pH 3.2. These results agree with those of Brady and Carroll [8] who found no direct dependence of labradorite dissolution on dissolved CO_2 at pH 4, although at much lower CO_2 pressure.

Labradorite temperature dependence

The temperature dependence of labradorite dissolution at constant pH and flow rate can be describe by the classical Arrhenius equation,

$$\text{Rate} = A \exp(E_a/RT) \qquad 1.$$

where A (mol cm^{-2} s^{-1}) is the pre-exponential factor, and E_a (kcal mol^{-1}) is the activation energy. We calculate the activation energy from the temperature dependence of labradorite dissolution

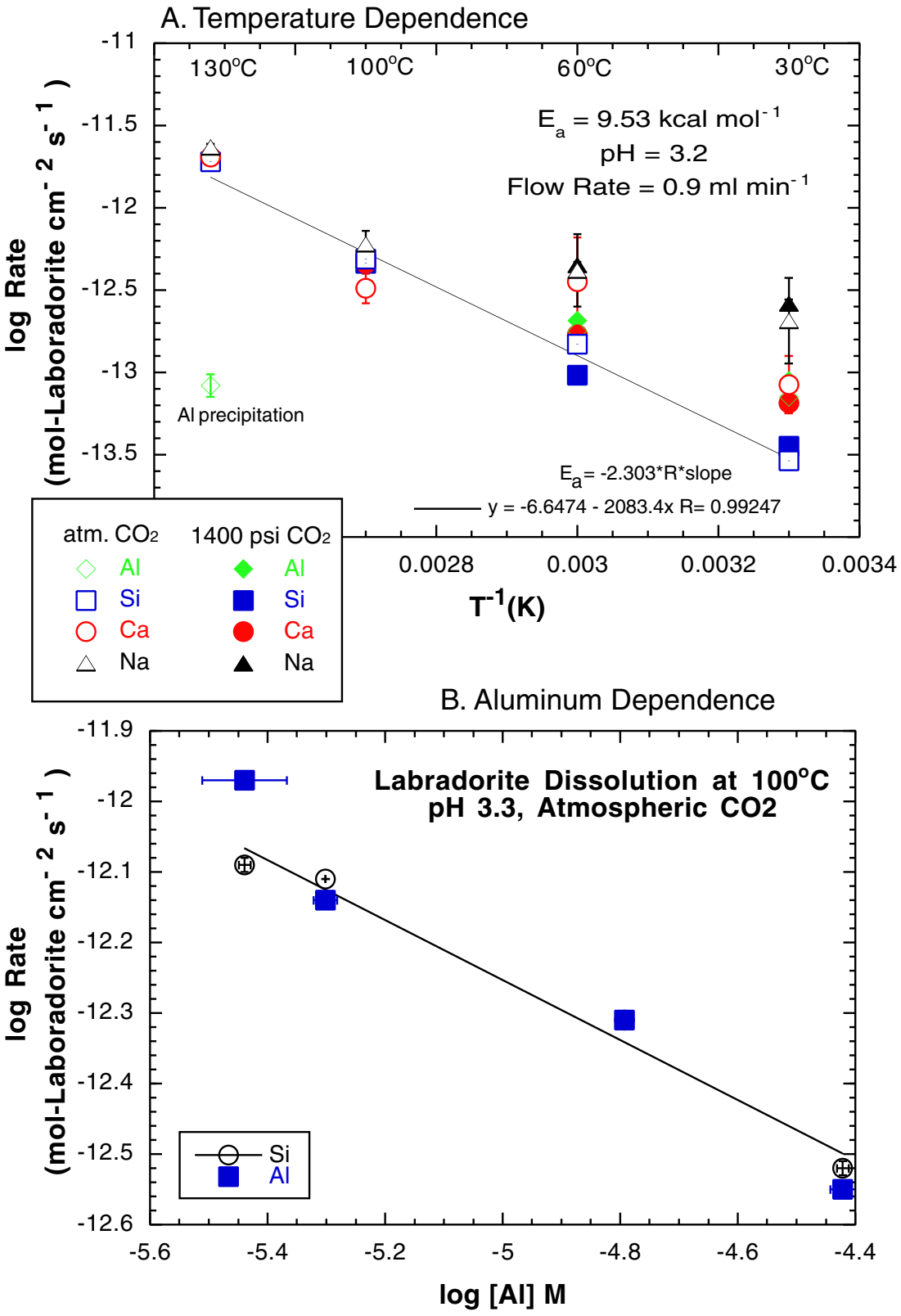

Figure 2. A. Labradorite dissolution at pH 3.2 in waters equilibrated with 1400 psi CO_2 (solid symbols) and with atmospheric CO_2 (open symbols) from 30 to 130°C. B. Labradorite dissolution at pH 3.3 in water equilibrated with atmospheric CO_2 100°C. Solid squares show the Al dissolution rate and the open circles show the Si dissolution rate. All rates are normalized to their mole equivalents in labradorite.

rates normalized to the silicon release at a constant flow rate (0.9 ml min^{-1}), because higher release rates of Na, Ca, and Al relative to silica were observed at 30 and 60°C. It is important that the temperature dependence be in terms of a constant flow rate at this point in our study, because labradorite dissolution appears to be affected by aqueous aluminum, which changes as a function of flow rate (see below). We calculate E_a = 9.53 (kcal mol^{-1}). This value is slightly lower than E_a ranging from 11.5 to 15.9 (kcal mol^{-1}) reported from other labradorite studies in acid solutions (pH 1-4, T 5-70°C) [9-11]. It's possible that modifying the overall rate expression to include the effect of aqueous aluminum on dissolution may account for the small discrepancy between our calculated activation energy and those from previous studies (see below).

Incongruent labradorite dissolution

Labradorite dissolution in water saturated with supercritical CO_2 can be describe by the following mass balance reaction:

$$Ca_{0.6}Na_{0.4}Al_{1.6}Si_{2.4}O_8 + 5.4H^+ + CO_{2(aq)} \Rightarrow$$

$$0.6Ca^{2+} + HCO_3^- + 2.2H_2O + 0.4Na^+ \; 1.6Al^{3+} + 2.4\; SiO_s(aq) \qquad 2.$$

Congruent dissolution would manifest itself as calcium, sodium, aluminum and silica rates that are proportional to their mole equivalents in labradorite. In our study we observe incongruent dissolution at 30 and 60˚C with enhanced release of sodium, calcium and aluminum over silicon release (Figure 2a). The rates are calculated from the constant concentration profiles from 20 to 140 hours. Presumably, we have reached steady-state, although it is possible that release of aluminum, calcium, and sodium would eventually be limited by the dissolution of the framework silica bonds and achieve congruent dissolution with time. We observe congruent dissolution only at 100˚C, because at higher temperature aluminum hydroxides, such as gibbsite, and potentially alumino-silicates, such as kaolinite, precipitate. These aluminum-bearing minerals precipitate at higher temperature because they have retrograde solubility in acid solutions which is related to the temperature dependence of aluminum hydrolysis [12]. At 130˚C we clearly see evidence for precipitation of an aluminum-bearing mineral from the aluminum dissolution rate, which is more

than 25 times lower than the silica dissolution rate. We conclude that the precipitate is an aluminum hydroxide and not an alumino-silicate because we see no evidence for removal of silica from the solution. We would expect to see incongruent dissolution with respect to calcium, sodium, and silica if an alumino-silicate precipitated from solution. This is not the case, labradorite dissolution rates at 130˚C are congruent for all elements (Ca, Na, and Si) except aluminum. We might also expect to see non-linear temperature dependence for the silica rates, if an alumino-silicate precipitated from solution at higher temperature (Figure 2). This is not the case. In fact we calculate the activation energy for labradorite dissolution from silica dissolution rates as a function of temperature.

Effect of aluminum on labradorite dissolution

The development of any rate equation to describe labradorite dissolution must include an expression that accounts for the observed decrease of alumino-silicate dissolution with increasing aluminum concentrations. We monitored this effect by conducting the dissolution experiments at different flow rates. The dissolve aluminum concentrations increase with decreasing flow rate, because the fluid residence time increases allowing more time for dissolution. At 100°C at pH 3.3 (atmospheric CO_2), labradorite dissolution decreases by a factor of 3 (0.5 log units) with a 10-fold increase in the aluminum concentration (Figure 2b). This phenomenon has been observed for alumino-silicate minerals in previous studies [13, 14]. At 100°C most of the experiments are supersaturated with respect to gibbsite and one at the lowest flow rate is supersaturated with respect to kaolinite. We cannot rule out the possibility that lower dissolution rates at higher aluminum concentrations are due to the precipitation of a secondary phase, but it seems unlikely. We observe congruent dissolution at all flow rates at 100°C and only the experiments with the highest aluminum concentrations are supersaturated with respect to kaolinite. If a secondary phase precipitates, we would expect to see incongruent dissolution with much lower aluminum concentrations, similar to our experiments at 130°C (Figure 2a). We are currently collecting additional rate data over a range of aqueous aluminum concentration to see if this relationship

holds at 30 and 60°C where dissolution is incongruent.

Dissolution and growth features on the labradorite surface

Figure 3 shows atomic force microscopy images and topography profiles of labradorite surface before and after the dissolution experiments. The unreacted surface is very smooth with less than 1 nm of vertical relief. The mineral cleavage planes are evident as striations across the image. The labradorite crystal was reacted in pH 3.2 waters for about one month in which bulk labradorite dissolution rates were measured in stacked runs at 30, 60, 100, and 130°C with flow rates ranging from .9 to 8.7 ml min^{-1}. The final run conditions were supersaturated with respect to gibbsite (an aluminum hydroxide) and kaolinite (a layered alumino-silicate). Therefore, we see both growth and dissolution features in Figure 3b. There are three important features that distinguish the reacted surface from the unreacted surface. An alteration layer covers the reacted mineral surface as is indicated by increased surface roughness of the reacted crystal (≈ 2 nm) and by the very muted image of the cleavage planes compared to the well developed striations in image of the unreacted crystal. This gel layer is thought to be a silica rich layer that polymerizes at the mineral-solution interface [6, 15-17]. Although the layer can be quite thick (30 nm at pH 2 and 125°C), in-situ hydrothermal atomic force microscopy studies indicate that dissolution is not limited by diffusion through this layer [6]. Once steady-state dissolution has been achieved (as in our experiments) the gel layer has reached a constant thickness, and mineral dissolution rates reflect reactions at the mineral surface. A second feature is the linear trend of dissolution pits that form along a cleavage ledge. These dissolution features are quite large with depths on the order of 50 nm. The third feature is the precipitation islands (presumably an aluminum hydroxide) that occur randomly on the surface. In some ways it is surprising that precipitation occurs randomly on the surface, and not along high energy sites found on the cleavage planes. This may be an artifact of the retrograde solubility of the aluminum hydroxides, which would create a more supersaturated solution as we rapidly increase the temperature from 100 to 130°C causing rapid nucleation of the aluminum hydroxide on the surface. Any subsequent growth

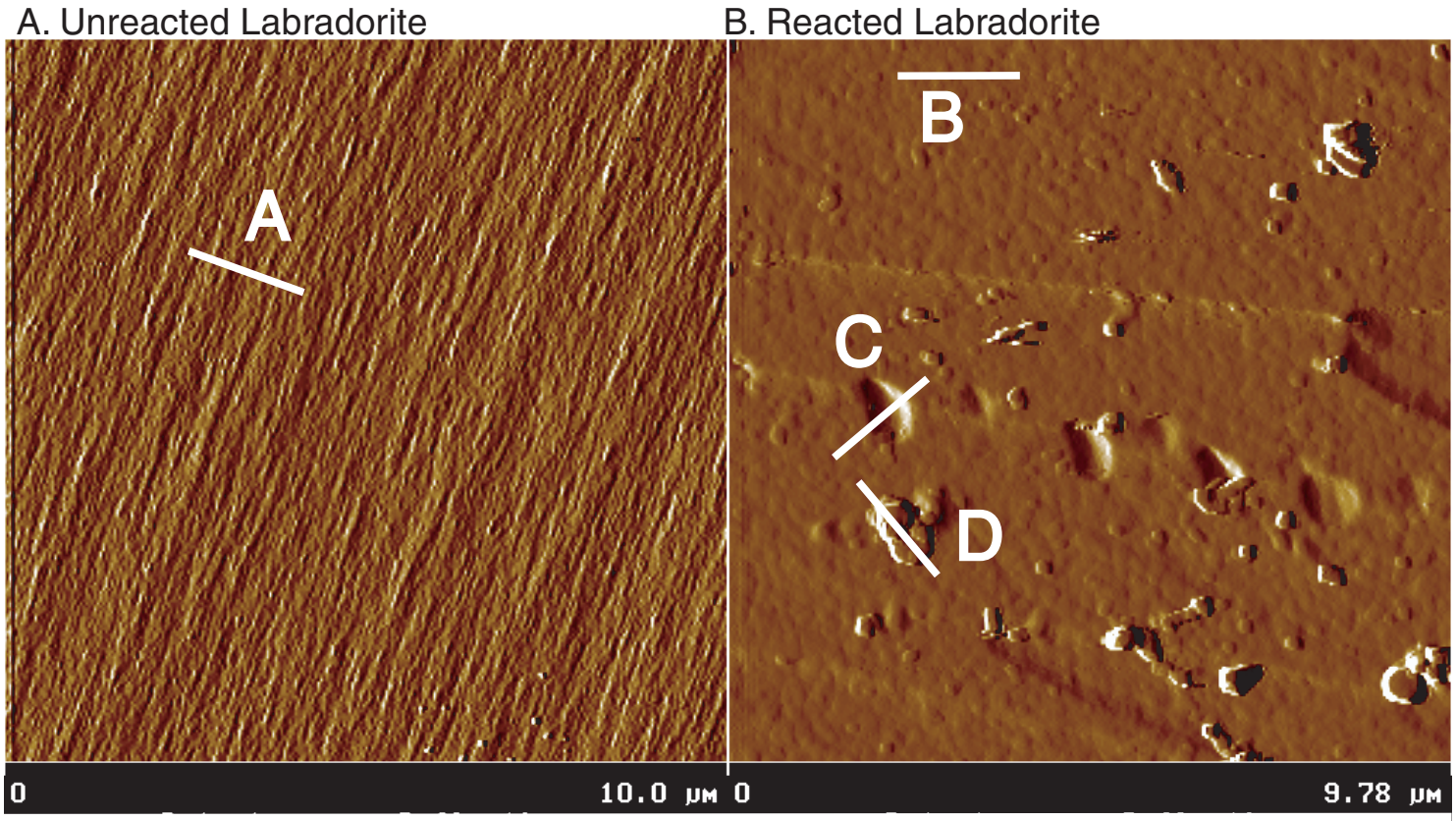

Figure 3. Atomic force microscopy images of the unreacted and reacted labradorite. Topographic profiles (A-D) are desribed in the text.

would occur at the surface of these precipitates as aluminum dissolves from labradorite.

Application

The focus of our work is to produce dissolution and precipitation rates needed to predict the reservoir capacity to effectively store CO_2 in the subsurface. Our work to-date has been concerned with measuring calcium-silicate dissolution rates at the reactive front where the injected supercritical CO_2 equilibrates with aquifer water. Towards this end we have already shown that high concentrations of dissolved CO_2 have no direct effect of mineral dissolution. Enhanced rates will be due to the increase in the acid concentration from the solubility of CO_2, over that due to low pH. At 60˚C and below, labradorite dissolution is incongruent with calcium rates as high as 3 times the silica rates. These rates appear to persist for long periods of time, and may need to be incorporated in CO_2 sequestration simulations to accurately predict the storage of CO_2 in carbonate minerals. Although the focus of our research so far has been on single dissolution studies, we have shown that secondary precipitation of aluminum phases occurs with increasing temperature. Injection and aquifer temperature are expected to be less than 100˚C. However, secondary precipitation will still be an important process downstream from the injection well (see **Future Activities**).

Future Activities

The next phase of our experiments will focus on coupled dissolution and precipitation reactions that occur downstream from the injection well. In this scenario, the waters are more neutral (pH 5 to 8) because dissolution of the aquifer rock has neutralized the acid, CO_2 rich waters. These experiments will focus on the precipitation rates of secondary carbonate, hydroxide, and alumino-silicate minerals. In this phase of the project, we will utilize the hydrothermal atomic force microscope to determine independent dissolution and precipitation rates, in conjunction with our continued use of the hydrothermal mixed flow reactor. Our kinetic research will feed directly into reactive transport codes that can evaluate aquifer storage of dissolved CO_2 as mineral carbonates, and resulting changes in porosity and permeability.

References

1. **Czernichowski-Laurio, I., Rochelle, C., Lindeberg E., Bateman, K, Sanjuan, B., *Analysis of the geochemical aspects of the underground disposal of CO2.* unpublished manuscript, (1994).**
2. **Butt, D.P., Lackner, K. S., Wendt, C. H., Conzone, S. D., Kung, H., Lu, Y.-C., Bremser, J. K., *Kinetics of thermal dehydroxylation and carbonation of magnesium hydroxide.* J. Am. Ceram. Soc., 1996. 79: p. 1892-1898.**
3. **Garrels, R.M., Mackenzie, F. T., *Evolution of Sedimentary Rocks*. 1971, New York: W.W. Norton & Co. 397.**
4. **Gunter, W.D., Wiwchar, B., Perkins, E. H., *Aquifer disposal of CO2-rich greenhouse gases: extension of the time scale of experiment for CO2-sequestering reactions by geochemical modeling.* Mineralogy and Petrology, 1997. 59: p. 121-140.**
5. **Higgins, S.R., Eggleston, C. M., Knauss, K. G., Boro, C. O., *A hydrothermal atomic force microscope for imaging in aqueous solutions up to 150C.* Rev. Sci. Instru., 1998. 69: p. 2994-2998.**
6. **Jordan, G., Higgins, S. R., Eggleston, C. M., Swapp, S. M., Janney, D. E., Knauss, K., *Acidic dissolution of plagioclase: In-situ observations by hydrothermal atomic force microscopy.* Geochim. Cosmochim. Acta, 1999. 63: p. 3183-3191.**
7. **White, A.F., Brantley, S. L., ed. *Chemical Weathering Rates of Silicate Minerals*. Reviews in Mineralogy, ed. P.H. Ribbe. Vol. 31. 1995, Mineralogical Society of America.**
8. **Brady, P.V., Carroll S. A., *Direct effects of CO_2 and temperature on silicate weathering: Possible implications for climate control.* Geochimica Cosmochimica Acta, 1994. 58: p. 1853-1856.**
9. **Sjoberg, L. *Kinetics and non-stoichiometry of labradorite dissolution*. In *Symposium on water-rock Interaction*. 1989: AA Balkema.**
10. **Brady, P.V., Walther, J. V., *Kinetics of quartz dissolution at low temperatures.* Chem. Geology, 1990. 82: p. 253-264.**
11. **Blum, A.E., Stillings, L. L., *Feldspar dissolution kinetics*, in *Chemical Weathering Rates of Silicate Minerals*, A.F. White, Brantley, S. L., Editor. 1995, Mineralogical Society of America. p. 291-351.**
12. **Bourcier, W.L., Knauss, K. G., Jackson, K. J., *Aluminum hydrolysis constants to 250C from boehmite solubility measurements.* Geochim. Cosmochim. Acta, 1993. 57: p. 747-762.**
13. **Chou, L., Wollast, R., *Study of the weathering of albite at room temperature and pressure with a fluized bed reactor.* Geochim. Cosmochim. Acta, 1984. 48: p. 2205-2217.**
14. **Oelkers, E.H., Schott, J., Devidal J. L., *The effect of aluminum, pH, and chemical affinity on the rates of aluminosilicate dissolution reactions.* Geochimica et Cosmochimica Acta, 1994. 58: p. 2011-2024.**
15. **Casey, W.H., Westrich, H. R., Arnold, G. W., *Surface chemistry of labradorite feldspar***

reacted with aqueous solutions at pH 2, 3, and 12. **Geochim. Cosmochim. Acta, 1988. 52: p. 2795-2807.**

16. **Casey, W.H., Westrich, H. R., Massis T., Banfield, J. F., Arnold, G. W., *The surface of labradorite feldspar after acid hydrolysis.* Chem. Geol., 1989. 78: p. 205-218.**
17. **Muir, I.J., Bancroft, G. M., Shotyk, W., Nesbitt, H. W., *A SIMS and XPS study of dissolving plagioclase.* Geochim. Cosmochim. Acta, 1990. 54: p. 2247-2256.**